Università di Pisa

Noise measurements in resonant tunneling structures as a function of current and temperature

P. Ciambrone
Dipartimento di Ingegneria dell'Informazione: Elettronica, Informatica, Telecomunicazioni, Università di Pisa
Massimo Macucci
Dipartimento di Ingegneria dell'Informazione: Elettronica, Informatica, Telecomunicazioni, Università di Pisa
Giuseppe Iannaccone
Dipartimento di Ingegneria dell'Informazione: Elettronica, Informatica, Telecomunicazioni, Università di Pisa
Bruno Pellegrini
Dipartimento di Ingegneria dell'Informazione: Elettronica, Informatica, Telecomunicazioni, Università di Pisa
M. Lazzarino
Laboratorio TASC-INFM, Trieste

A. Annovi, M.G. Bagliesi, A. Bardi, R. Carosi, M. Dell'Orso, M. D'Onofrio, P. Giannetti, G. Iannaccone, F. Morsani, M. Pietri, G. Varotto, *The fast tracker processor for hadron collider triggers*, IEEE Transactions Nuclear Science, **48**(3), p. 575 (2001).

L. Sorba
Laboratorio TASC-INFM, Trieste
F. Beltram
Laboratorio TASC-INFM, Trieste

P. Ciambrone, M. Macucci, G. Iannaccone, B. Pellegrini, M. Lazzarino, L. Sorba, F. Beltram, *Noise measurements in resonant tunneling structures as a function of current and temperature* , Electronics Letters, **31**, pp.503-504 (1995).

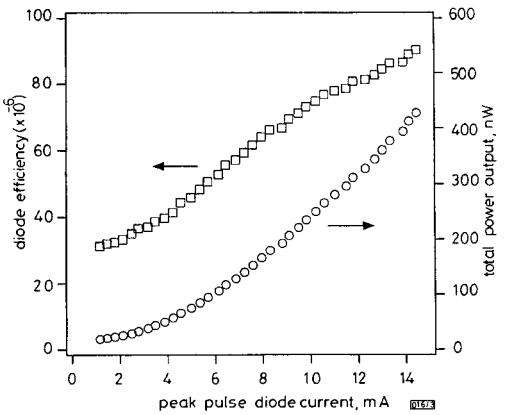

Fig. 3 *Total power output and external diode efficiency against injected peak current (50% duty cycle, 300K)*

□ external diode efficiency
○ total output power

In conclusion, we have reported, to our knowledge for the first time, electroluminescence from InGaAs/InAlAs LEDs lattice-mismatched grown on GaAs substrates. We have demonstrated that using MBE it is possible to grow high-quality material and also that the composition of the layers can be tuned to the desired wavelength. This should open up new possibilities to use infra-red LEDs in gas sensors.

Acknowledgments: The authors thank W. Va De Graaf for his excellent support in growing the samples. This work is funded by the 'Vlaams Instituut voor de bevordering va het wetenschappelijk-technologisch onderzoek in de industrie (IWT)' and the 'Nationaal Fonds voor Wetenschappelijk Onderzoek (NFWO)'.

20 January 1995
Electronics Letters Online No: 19950325

B. Grietens, M.R. Murti, C. Van Hoof and G. Borghs (*IMEC, Kapeldreef 75, B-3001 Leuven, Belgium*)

References

1 MCCABE, S., and MACCRAITH, B.D.: 'Novel mid-infrared LED as a source for optical fibre gas sensing', *Electron. Lett.*, 1993, **29**, pp. 1719–1721

2 MAJOR, J.S. Jr., NAM, D.W., OSINSKI, J.S., and WELCH, D.F.: 'High-power single-mode 2.0μm laser diodes', *IEEE Photonics Technol. Lett.*, 1993, **5**, pp. 733–734

3 FOROUHAR, S., KEO, S., LARSSON, A., KSENDZOV, A., and TEMKIN, H.: 'Low threshold continuous operation of InGaAs/InGaAsP quantum well lasers at ~2.0μm', *Electron. Lett.*, 1993, **29**, pp. 574–576

4 DOBBELAERE, W., DE BOECK, J., BRUYNSERAEDE, C., MERTENS, R., and BORGHS, G.: 'InAsSb light-emitting diodes and their applications to infra-red gas sensors', *Electron. Lett.*, 1993, **29**, pp. 890–891

5 PARRY, M.K., and KRIER, A.: 'Efficient 3.3μm light-emitting diodes for detecting methane gas at room temperature', *Electron. Lett.*, 1994, **30**, pp. 1968–1969

6 WADA, M., and HOSOMATSU, H.: 'Wide wavelength and low dark current lattice-mismatched InGaAs/InAsP photodiodes grown by metal-organic vapour-phase epitaxy', *Appl. Phys. Lett.*, 1994, **64**, pp. 1265–1267

7 LINGA, K.R., JOSHI, A.M., BAN, V.S., and MASON, S.: '1024 element linear $In_xGa_{1-x}As/InAs_yP_{1-y}$ detector-arrays for environmental sensing from 1μm to 2.6μm'. Proc. SPIE, 1993, Vol. 2021, pp. 90–97

8 FISCHER-COLBRIE, A., JACOWITZ, R.D., and AST, D.G.: 'Non-lattice matched growth of $In_xGa_{1-x}As$ ($0.53<x<0.80$) on InP', *J. Cryst. Growth*, 1993, **127**, pp. 560–565

9 DOBBELAERE, W., BOECK, J.D., HEREMANS, P., MERTENS, R., BORGHS, G., LUYTEN, W., and LANDUYT, J.V.: '$InAs_{0.85}Sb_{0.15}$ infrared photodiodes grown on GaAs and GaAs-coated Si by molecular beam epitaxy', *Appl. Phys. Lett.*, 1992, **60**, pp. 3256–3258

10 WESTWOOD, D.I., WOOLF, D.A., and WILLIAMS, R.H.: 'Growth of $In_xGa_{1-x}As$ on GaAs(001) by molecular beam epitaxy', *J. Cryst. Growth*, 1989, **98**, pp. 782–792

Noise measurements in resonant tunnelling structures as a function of current and temperature

P. Ciambrone, M. Macucci, G. Iannaccone, B. Pellegrini, M. Lazzarino, L. Sorba and F. Beltram

Indexing terms: Resonant tunnelling devices, Semiconductor device noise

The authors present the results of noise measurements performed on custom designed resonant tunnelling structures. The shot-noise suppression has been measured as a function of bias current and temperature in the 14 – 223K range, and results have been compared with those predicted by existing theories.

Introduction: Shot-noise suppression in resonant-tunnelling double-barrier structures (RTDBSs) has recently attracted the interest of device physicists and electrical engineers. While several theoretical attempts at explaining this phenomenon have been made [1 – 4], very few experimental data are available in the literature [4, 5]. Further investigation of this problem is needed, because theoretical and experimental results do not provide a fully consistent picture.

A few authors have argued that shot-noise suppression would be maximum for equal transmission coefficients of the two barriers [1 – 3]; therefore, we have designed, fabricated and tested a resonant tunnelling diode able to satisfy this condition for a proper value of the applied bias voltage.

Experimental conditions: The sample was grown by molecular beam epitaxy (MBE) on *n*-doped GaAs (001) substrate ($10^{18}cm^{-3}$) with the following layer structure: a silicon doped ($n = 1.4 \times 10^{18}cm^{-3}$) 500nm-thick GaAs buffer layer, an undoped 20nm-thick GaAs spacer layer to prevent silicon diffusion into the barrier, an undoped 11.5nm-thick $Al_{0.36}Ga_{0.64}As$ first barrier, an undoped 5nm-thick GaAs quantum well, an undoped 10nm-thick $Al_{0.36}Ga_{0.64}As$ second barrier, an undoped 15nm-thick GaAs spacer layer and a silicon-doped ($n = 1.4 \times 10^{18}cm^{-3}$) 500nm-thick GaAs cap layer to realise the emitter terminal.

The barriers have equal heights but different thicknesses, to achieve maximum symmetry of transmission coefficients for a bias voltage of 0.2 – 0.3V. The asymmetry of the two spacer layers is due to the greater diffusion coefficient of the dopant in the growth direction.

Ohmic contacts were defined by photolithography on the top layer and used as stop-etches to define the emitter circular mesas with a diameter of 50μm. The collector contact was formed by metallising the whole substrate base.

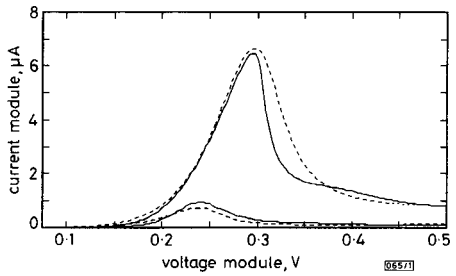

Fig. 1 *Comparison between simulated and experimental I/V characteristic at 77K for forward and reverse bias*

- - - - simulated
——— experimental
upper curves: forward bias
lower curves: reverse bias

Fig. 1 shows a comparison between experimental results and the outcome of numerical simulations for forward- and reverse-bias I/V curves at 77K. The agreement between theoretical and experimental curves gives us confidence about the correspondence between nominal and actual values of barrier parameters. Theoretical curves have been obtained with the inclusion of dissipation by means of a phenomenological relaxation time.

Our samples have been cooled down in a two-stage helium expansion cryostat that has been custom-modified to reduce vibrations of the sample holder. The sample holder is mechanically independent from the cooling stages, while heat transmission is provided by a gaseous helium cushion. Vacuum in the sample chamber is obtained with a hydrocarbon-free dry pumping system.

Noise measurements have been performed with a recently developed technique [6], allowing an accurate estimate of spurious contributions from the input amplifier and from the biasing network. These contributions can thus be subtracted from the total noise spectrum.

Results: Most of our measurements have been performed in a frequency range between 100Hz and a few kilohertz, where the noise spectrum is substantially flat. Below 100Hz flicker noise contributions become significant, particularly for the higher current bias values, and above a few kilohertz the equivalent input current noise of the amplifier is prevalent.

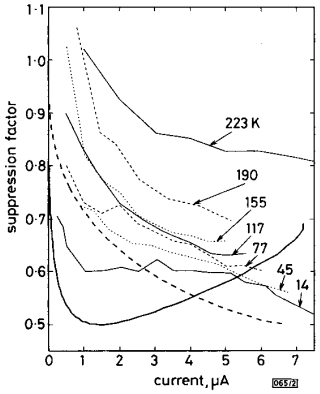

Fig. 2 *Shot-noise suppression factor against bias current for different temperatures*

Thick curves represent theoretical result of [1 – 3], computed using effective mass of [7], (– – –) and of [8], (——)

In Fig. 2 we report the noise suppression factor (averaged over the above-mentioned frequency range) as a function of bias current for several different temperatures. The noise suppression factor is defined as the ratio of the measured noise level S_I to the theoretical full shot-noise $S_{IF} = 2qI$, where q is the electron charge and I is the bias current. There is a clear trend towards a decrease of the suppression effect with increasing temperature. We also notice that for the lowest temperature (14K) the shot-noise suppression factor approaches a value of 0.5 for current values near the peak. We compare these experimental results with a well known theoretical model [1 – 3], according to which the shot-noise suppression factor should be equal to $1-T_{res}/2$, where T_{res} is the transmission coefficient of the whole structure at the resonant energy, in the hypothesis of coherent transport. We report the calculation of $1-T_{res}/2$ for two different values of the effective mass m^* in the barriers: the thick broken line corresponds to $m^*/m_0 = 0.067 + 0.083x$ in $Al_xGa_{1-x}As$ [7], while the thick solid line is obtained for an effective mass ($m^*/m_0 = 0.08$) obtained from the interpolation between the value of m^* in GaAs and that in AlAs proposed by [8]. The first theoretical curve approaches the trend of the experimental data; however, it is clear from a comparison between the two curves that the model is highly sensitive to the choice of the effective mass value, whose actual validity is debatable in structures with very thin layers.

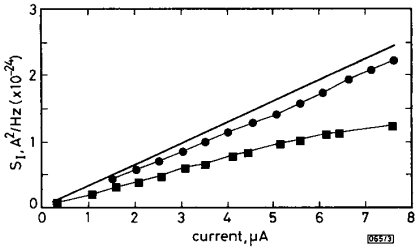

Fig. 3 *Power spectral density of current noise at 14K against bias current for positive differential resistance region before and beyond the peak*

■ before peak
● beyond peak
—— full shot-noise value

In Fig. 3 we show the shot-noise power spectral density as a function of current at 14K in the positive differential resistance regions before and after the direct bias peak. We notice that beyond the peak no substantial suppression can be observed. A similar result has been obtained also at the other temperatures.

Conclusion: The shot-noise suppression in an RTDBS has been measured as a function of current bias for several values of temperature. Our results have been compared with predictions from a theoretical model, obtaining a qualitative agreement for a particular choice of the effective mass. However, we do not consider this agreement as a proof of the validity of the model, because of the high sensitivity to the effective mass value. Moreover, this model has been demonstrated for purely coherent transport, which is not expected to be prevalent in these devices, even at very low temperatures. Therefore we are planning to perform noise measurements on a set of devices with different thicknesses for the collector barrier and to include in the theory noncoherent and dissipative effects.

Acknowledgments: The third author is grateful for useful discussions with G.C. Aers, C.R. Leavens and H.C. Liu. This work has been supported by the Italian Ministry of University and Scientific and Technological Research and by the Italian National Research Council (CNR).

25 January 1995
Electronics Letters Online No: 19950315

P. Ciambrone, M. Macucci, G. Iannaccone and B. Pellegrini (*Dipartimento di Ingegneria dell'Informazione: Elettronica, Informatica, Telecommunicazioni, Università degli Studi di Pisa, Via Diotisalvi, 2, I-56126 Pisa, Italy*)

M. Lazzarino, L. Sorba and F. Beltram (*Laboratorio TASC-INFM, 34012 Trieste, Italy*)

References

1 CHEN, L.Y., and TING, C.S.: 'Theoretical investigation of noise characteristics of double-barrier resonant-tunneling systems', *Phys. Rev. B*, 1992, **46**, pp. 4714–4717

2 BÜTTIKER, M.: 'Role of scattering amplitudes in frequency-dependent current fluctuations in small conductors', *Phys. Rev. B*, 1992, **45**, pp. 3807–3810

3 DAVIES, J.H., HYLDGAARD, P., HERSHFIELD, S., and WILKINS, J.W.: 'Classical theory of shot noise in resonant tunneling', *Phys. Rev. B*, 1992, **46**, pp. 9620–9633

4 BROWN, E.R.: 'Analytic model of shot noise in double-barrier resonant-tunneling diodes', *IEEE Trans.*, 1992, **ED-39**, pp. 2686–2693

5 LI, Y.P., ZASLAVSKY, A., TSUI, D.C., SANTOS, M., and SHAYEGAN, M.: 'Noise characteristics of double-barrier resonant-tunneling structures below 10kHz', *Phys. Rev. B*, 1990, **41**, pp. 8388–8391

6 MACUCCI, M., and PELLEGRINI, B.: 'Very sensitive measurement method of electron device current noise', *IEEE Trans.*, 1991, **IM-40**, pp. 7–12

7 CASEY, H.C., and PANISH, M.B.: 'Heterostructure lasers' (Academic, New York, 1978), Part A, Chap. 4

8 LANDHEER, D., LIU, H.C., BUCHANAN, M., and STONER, R.: 'Tunneling through AlAs barriers: Γ-X transfer current', *Appl. Phys. Lett.*, 1989, **54**, (18), pp. 1784–1786

Q-band high-efficiency monolithic HEMT power prematch structures

R. Kasody, H. Wang, M. Biedenbender, L. Callejo, G.S. Dow and B.R. Allen

Indexing terms: High-electron-mobility transistors, Impedance matching

Monolithic Q-band high-efficiency prematch structures using 0.15 μm double-heterostructure pseudomorphic AlGaAs/InGaAs/GaAs HEMTs have been designed, fabricated and evaluated. The structures include a 400μm and an 800μm gate-width unit, demonstrating power-added efficiency of 41.6% and 37%, respectively, which represents state-of-the-art efficiency performance at this frequency. These building blocks can be used easily to construct high-power, high-efficiency amplifiers. The circuit design, output power and efficiency performance of the prematch structures are also presented.

Introduction: There are increasing demands for the performance of high-efficiency millimetre-wave power amplifiers (PAs) in various system applications. Quite a few Q-band (44GHz) high-power, high-efficiency monolithic amplifiers and power devices have been reported using either GaAs- or InP-based HEMT devices [1 – 5]. Recently, Chen *et al.* reported a 1W monolithic two-stage power amplifier (PA) [3], while Smith *et al.* reported a 1.8mm-gate-width device with 800mW output power and 25% power-added efficiency (PAE) [4] at 44.5GHz, and Huang *et al.* reported 38% PAE of a 400 μm-gate-width device [3] at 44GHz, using 0.15μm-gate GaAs-based HEMTs. The InP HEMT devices demonstrate a higher PAE of 31% for a single-stage MMIC PA with 630mW output power on a 2mil substrate [5].

This Letter presents two high-efficiency 44GHz monolithic HEMT prematch structures (indeed single-stage MMIC amplifiers) using a 0.15μm passivated T-gate pseudomorphic InGaAs channel HEMT fabrication process on a 4mil GaAs substrate. One employs 400μm-gate-width device, and the other has 800μm gate width. These structures demonstrate the highest PAE for the size of these devices ever reported at this frequency: 41.6% for the 400μm unit and 37% for the 800μm unit. The prematch structures can be used as building blocks to construct monolithic high-power amplifiers easily, which overcomes the difficulty of matching the low impedance for a large periphery power device in the PA design. This design approach has demonstrated successfully state-of-the-art high-performance MMW PAs in the Ka-band (35 GHz) [6] and V-band (60GHz) [7].

Device characteristics and circuit design: The PM HEMT devices employ a double-heterostructure layer design and are similar to devices reported earlier [3, 6, 7]. The devices exhibit a maximum transconductance greater than 500mS/mm and a maximum current density greater than 600mA/mm. The gate-to-drain breakdown voltage defined at 1mA/mm is typically greater than 10V. The devices also demonstrate a very low output conductance of less than 25mS/mm and excellent pinch-off characteristics. The typical unit current gain cutoff frequency f_T is 90GHz and maximum oscillation frequency f_{max} is 200GHz for an 80μm-gate-width device.

Fig. 1 shows the layout of the 44GHz 400μm and 800μm monolithic prematch units with chip sizes of 2.4 × 1.0 and 2.4 × 1.55mm², respectively. These structures are based on a 4mil-thick GaAs substrate. They both consist of common source four-finger 200μm cells combined in parallel to form the 400μm and 800μm HEMT devices with the via holes placed between each two adjacent 200μm cells. Cascaded high/low-impedance microstrip lines are used to form the input and output matching networks. The two-section quarter-wave impedance transformers match the input

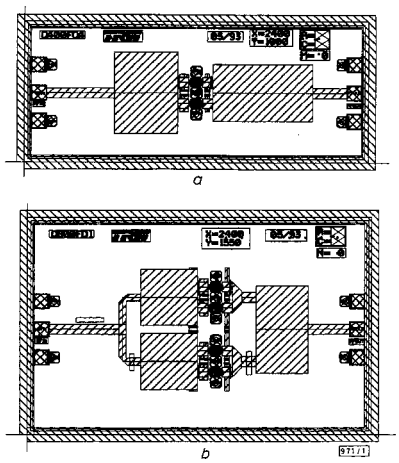

Fig. 1 *Layout plots of 44GHz monolithic 400μm and 800μm prematch structures*

a 400μm
b 800μm

and output from low impedances looking into the common source HEMT devices to 50Ω. Thin-film resistors are added to each two adjacent 200μm cells to prevent odd-mode oscillation. The chip accommodates 200μm pitch ground-signal-ground connecting pads to allow on-wafer testing. The prematch structures can be used as building blocks to construct monolithic high-power amplifiers easily, which overcomes the difficulty of matching the low impedance for a large periphery power device in the PA design.

Measurement results: These prematched structures were tested on-wafer for small-signal gain first. The small-signal gain is 9dB for the 400μm unit and 8dB for the 800μm unit. Both the prematch structures were mounted in a Q-band fixture for power performance evaluation. Antipodal finline transitions on a 3mil-thick fused silica substrate are used to couple the signal from the waveguide to the microstrip. Quarter-wavelength lines plus wide-open stubs for RF ground were added on the microstrip transmission lines in the test fixture for biasing. The typical insertion loss of this transition fixture with back-to-back transition connections is 1dB. All the data presented below have been corrected by 0.5 dB for both input and output transition.

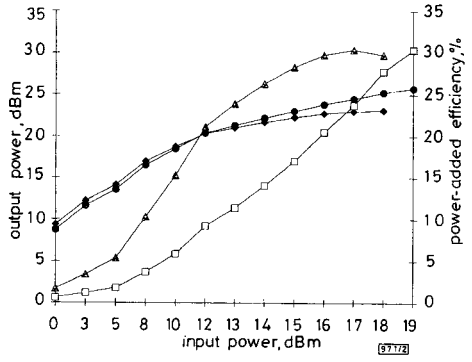

Fig. 2 *Output power and PAE against input power plots for both prematch amplifiers at 44GHz biased for maximum output power*

Fig. 2 plots output power and efficiency against input power at 44GHz for both prematch amplifiers with a drain voltage of 5V. Output powers of 23 and 25.8dBm were obtained for the 400 and 800μm units, respectively, with the same PAE of 30.4%. However, for the lower drain bias, we observed a PAE of 34.3% at 3.5V drain bias for the 400μm unit and 4V drain bias for the 800μm unit. By further adjusting the tuning pads around the output